Current Biology, Volume *32*

Supplemental Information

Unique spatiotemporal fMRI dynamics in the awake mouse brain

Daniel Gutierrez-Barragan, Neha Atulkumar Singh, Filomena Grazia Alvino, Ludovico Coletta, Federico Rocchi, Elizabeth De Guzman, Alberto Galbusera, Mauro Uboldi, Stefano Panzeri, and Alessandro Gozzi

SUPPLEMENTAL FIGURES

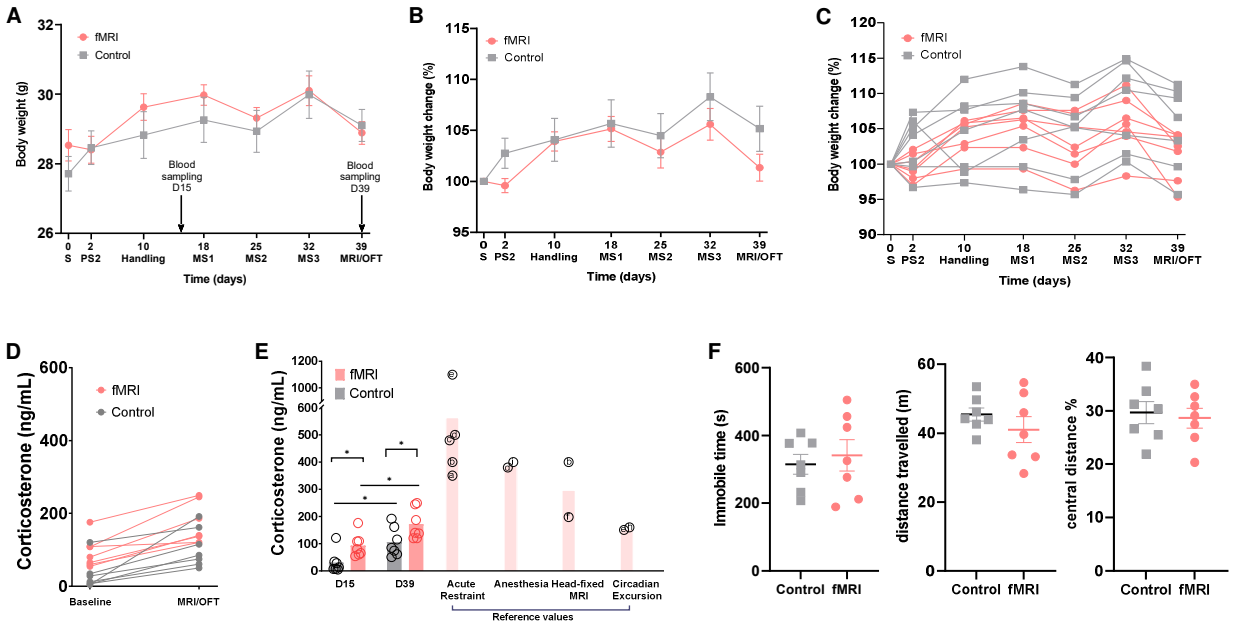

Figure S1. Stress monitoring during habituation for awake MRI imaging. A) Body weight measurements over the 4 weeks of habituation protocol (fMRI group, N =7, Control, n = 7). [Day 0 S, before surgery; day 2 PS2, 2 days post-surgery; day 10 Handling, first day of habituation procedure; day 18 MS1, first day of mock scanning session 1; day 25 MS2, first day of mock scanning session 2; day 32 MS3, first day of mock scanning session 3]. Arrows indicate time of blood sampling for corticosterone measurements (D15 and D39). **B)** Percentage change in body weight over the course of the habituation protocol at the group and **C)** subject level. **D)** Plasma corticosterone concentration (ng/mL) at the end of the handling week (fMRI group) or during homecage housing (Control), and right after fMRI scanning (fMRI group) or after open field behavioral testing (control group). **E)** The same values in D) are reported here with respect to representative plasma corticosterone levels reported in the mouse literature upon acute restraint, anesthesia induction, head-fixed MRI. Circadian excursion levels are also reported for reference. [Acute Restraint: a: [62], b: [63], c: [64], d: [65], e: [49], Anesthesia: d, i: [66], Head-fixed MRI: b, f, [67], g, [68]; Circadian Excursion: e, h: [69]]. **F)** Time Immobile (seconds, s), distance travelled (meters, m) and percentage of distance travelled in the central zone of the arena in the open field test by mice belonging to the awake fMRI and control littermate groups. Data are expressed as mean ± SEM.

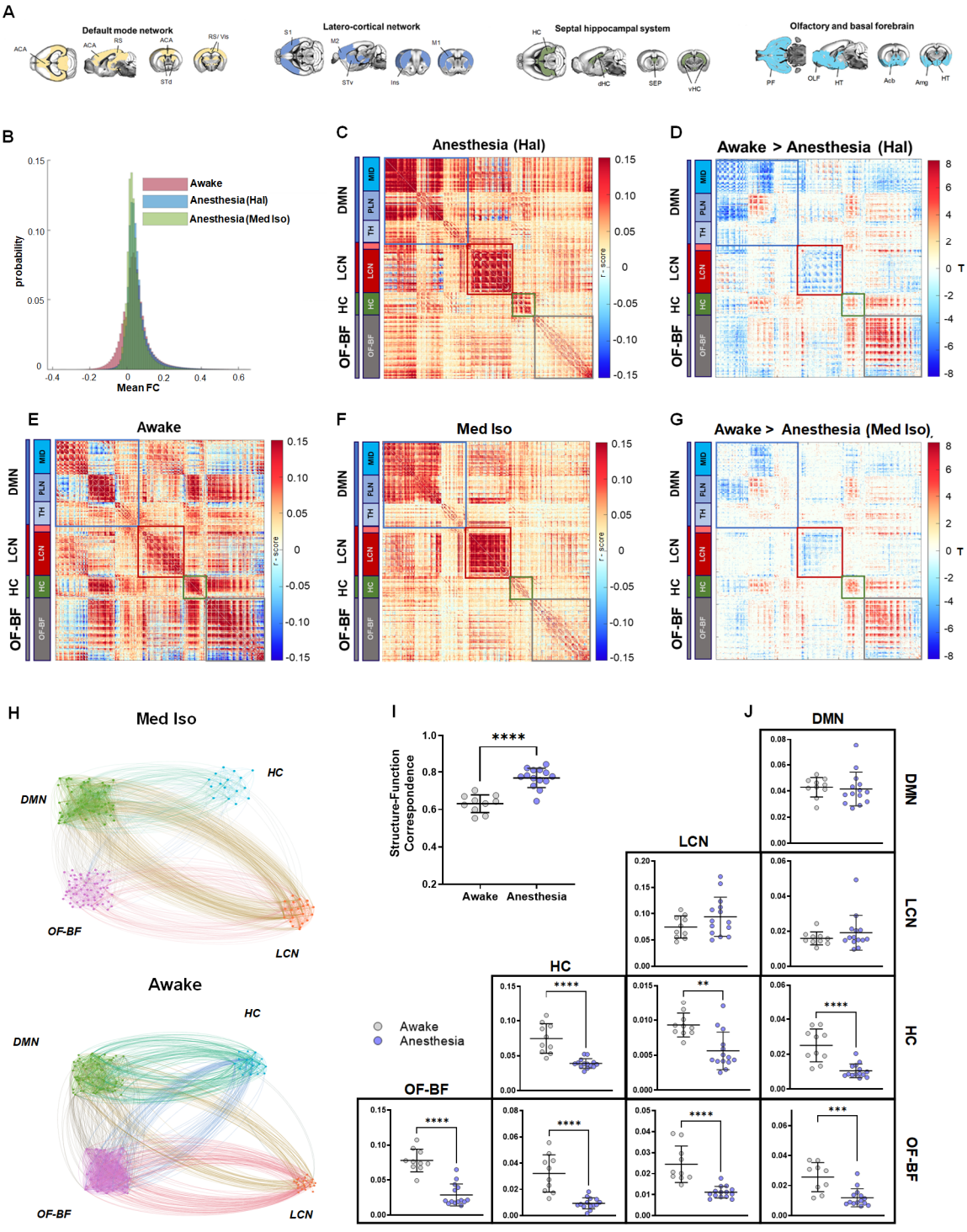

Figure S2. Voxel-wise connectivity and structure-function relationship in medetomidine-isoflurane (Med Iso) anesthetized mice. A) Axonal connectivity modules in the mouse brain spatially reconstitute macro-scale networks of the mouse brain (replicated with permission from Coletta et al., 2020). **B)** Distribution of mean functional connectivity in awake and anesthetized mice. Note the larger proportion of negative correlation in awake state. **C-G)** Group averaged voxel-wise FC matrices in awake **E)** and two independent anesthesia conditions (Halothane and Med Iso, C and F, respectively) with voxels organized within axonal connectivity modules, and further partitioned into network sub-modules. The sub-module corresponding to the thalamic voxels within the LCN module are not labeled (light-red block). Significant between-state FC differences at the voxel

level (two-tailed two-sample T-test) for Halothane (D) and Med Iso (G) show consistent deviations from the awake state. **H)** Graphic representation of rsfMRI connectivity within and between previously described axonal modules of the mouse brain (DMN, LCN, HC, OF-BF, from Coletta et al., 2020). Each cluster of nodes represents a subset of anatomically-defined ROIs within the corresponding module. Nodes have been empirically arranged to maximize figure legibility. **I)** Structure-function correspondence in awake and Med Iso anesthetized mice. Between-group differences were assessed with a Mann-Whitney test ($p < 0.05$). **J)** Quantification of within (diagonal) and between (off-diagonal) network functional connectivity (*p<0.05, ** p<0.01, *** p<0.001, **** p<0.0001, Mann-Whitney test, FDR corrected). [DMN: Default mode network, HC: Hippocampus, OF-BF: Olfactory and basal forebrain, LCN: latero-cortical network].

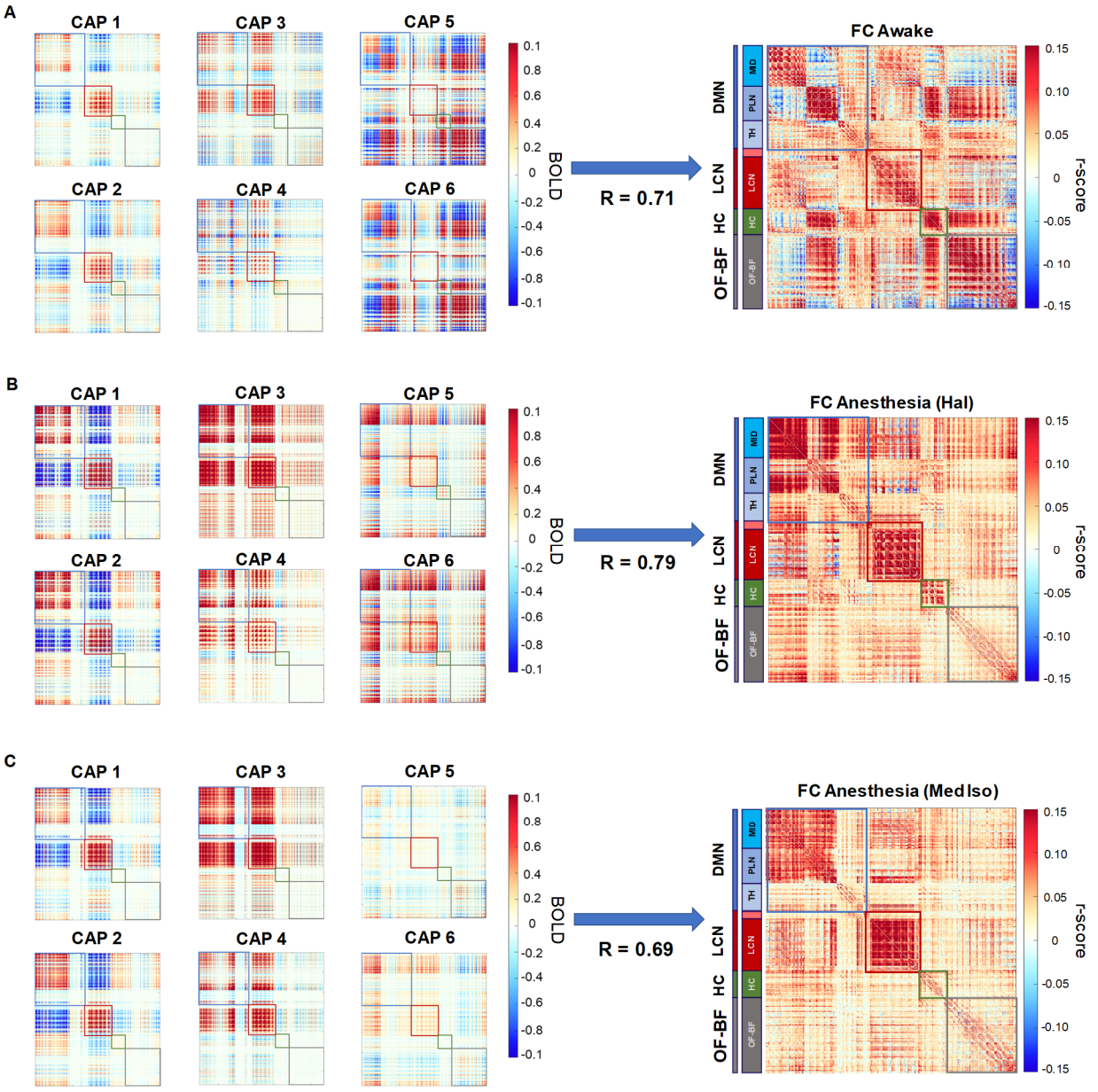

Figure S3. CAPs explain a large fraction of variance in the static functional connectome. Co-fluctuation matrices (left) computed by cross-multiplying each group-mean CAP map with itself, and corresponding time-averaged functional connectivity matrices (right) in awake (top) and anesthetized (Halothane-middle, and Med Iso-bottom) mice. Averaged co-fluctuation matrices (CAPs 1-6) exhibit a correlation of 0.71, 0.79, and 0.69 with the corresponding stationary functional connectome in awake (A), halothane anesthesia (B) and Med Iso, respectively.

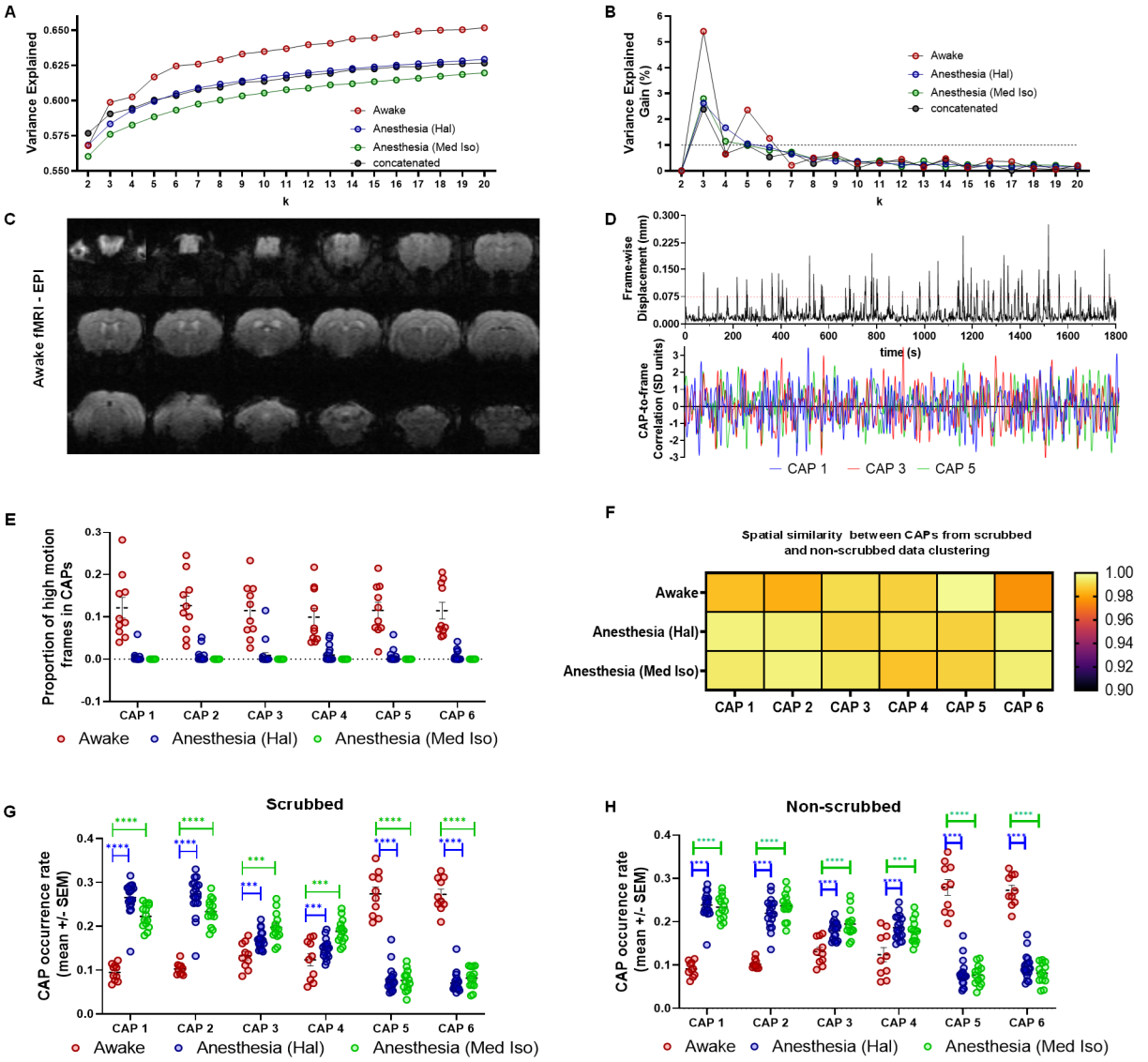

Figure S4. Data-clustering selection and effect of scrubbing high-motion frames. A) Variance explained by clustering each dataset independently and after concatenating all datasets with k = 2:20. **B)** Percentage gain in variance explained when advancing from k-1 to k. The black dashed line indicates the 1% gain. **C)** Raw EPI from a randomly selected subject from the awake group (mid-scan frame). **D)** Frame-wise displacement (in mm) summarizing instantaneous head-motion (top) from the mouse depicted in (C) and CAP-to-frame correlation time course (bottom) for the same mouse (odd-CAPs shown). **E)** Proportion (Mean± SEM) of motion-flagged (FD > 0.075 mm) fMRI frames that were clustered within a CAP. There are no significant differences between CAPs (ANOVA $p > 0.92$) for all groups. **F)** Spatial correlations between CAPs obtained from independent clustering (k=6) with and without scrubbing frames with FD > 0.075mm. Each row shows the correlation for the group-averaged CAP maps. Spatial correlation was > 0.96 for all CAP pairs. **G-H)** CAP occurrence rates are not affected by motion. Quantification of CAP occurrence rates (Mean± SEM) in awake and anesthetized mice with **(G)** and without **(H)** fMRI frame scrubbing**.** (***$p < 0.001$, ****$p < 0.0001$, Two-tailed, two-sample T-test, FDR corrected for six comparisons).

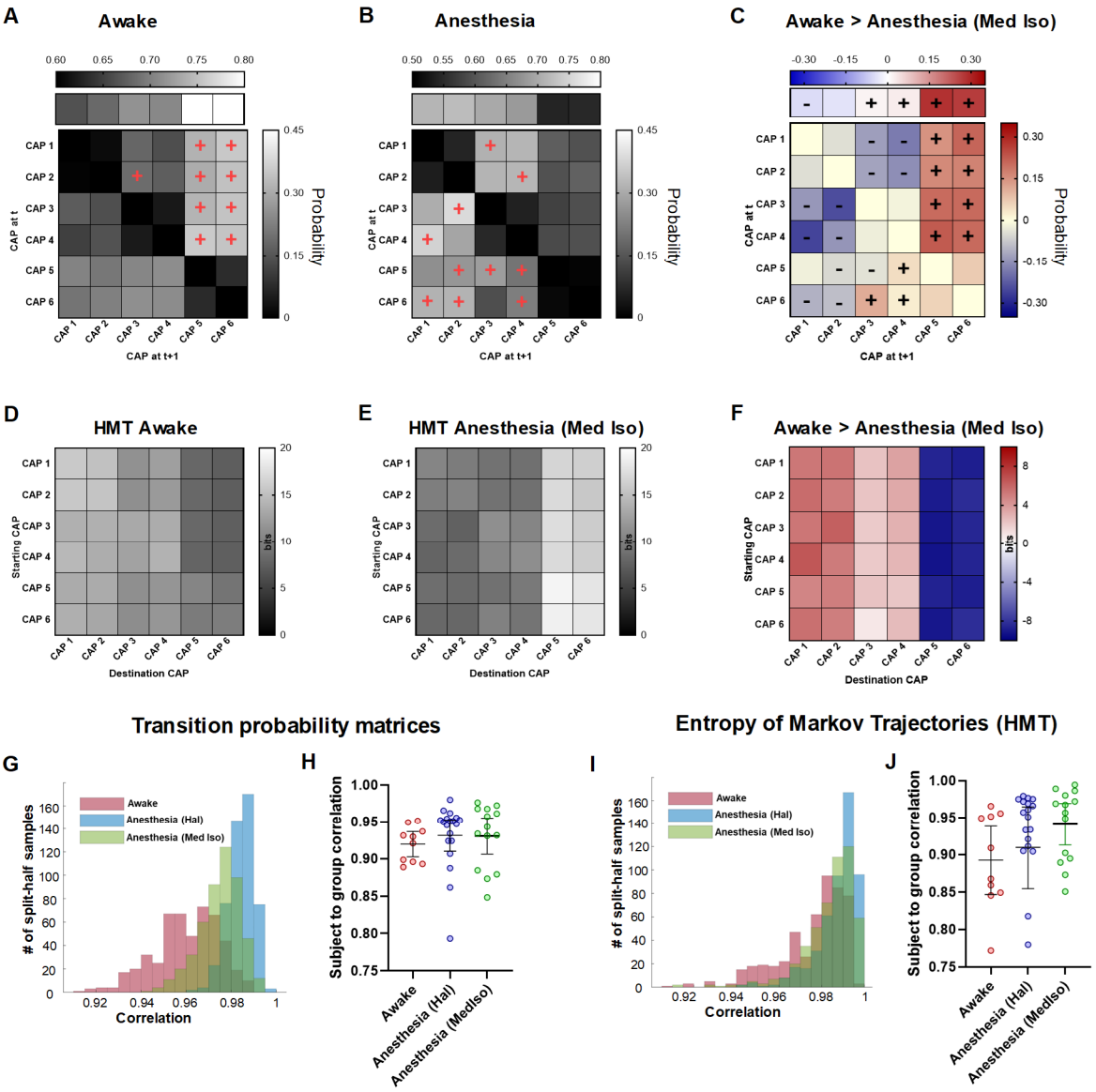

Figure S5. Conserved CAP transition probabilities and preferred trajectories under medetomidine isoflurane anesthesia. A-B) Persistence (top row) and transition (off-diagonal) probabilities in awake (A) and Med Iso anesthetized (B) mice. Persistence probabilities are all significant (above null elements from matrices built from 1000 randomly and uniformly permuted sequences not accounting for repetitions). Significant preferred transitions $P_{ij} > P_{ji}$ are denoted with a red "+" sign. Directional transitions are depicted if the incoming transition P_{ij} is significant (above null elements from matrices built from 1000 randomly and uniformly permuted sequences without repetitions). **C)** Transition probability differences between groups are denoted with a "+" sign for transitions higher in awake, and conversely with a "-" sign, if higher in anesthesia. Persistence probability differences were tested with permuted CAP sequences that included repeating elements. **D-E)** Entropy of Markov trajectories (HMT) in awake (D) and anesthetized mice (E). **F)** Corresponding state-dependent differences in HMT (all elements show significant differences, above and beyond 1000 randomly and uniformly permuted CAP sequences without repetitions). Positive elements represent CAP trajectories with lower accessibility in the awake state as compared with anesthesia, while negative elements are trajectories with facilitated access in awake state. Only the path from CAP 6 to CAP 2 showed non-significant differences. **G)** Distribution of Pearson's correlation scores between the mean group transition probabilities and the ones obtained after 500 split-half resampling of random subjects within each condition. **H)** Correlations between single subject transition probability matrices and the mean group one. **I)** Distribution of Pearson's correlation scores between the mean group Entropy of Markov Trajectories matrix and the ones obtained after 500 split-half resampling of random subjects within each condition. **H)** Correlations between single subject Entropy of Markov Trajectories matrices and the mean group one.

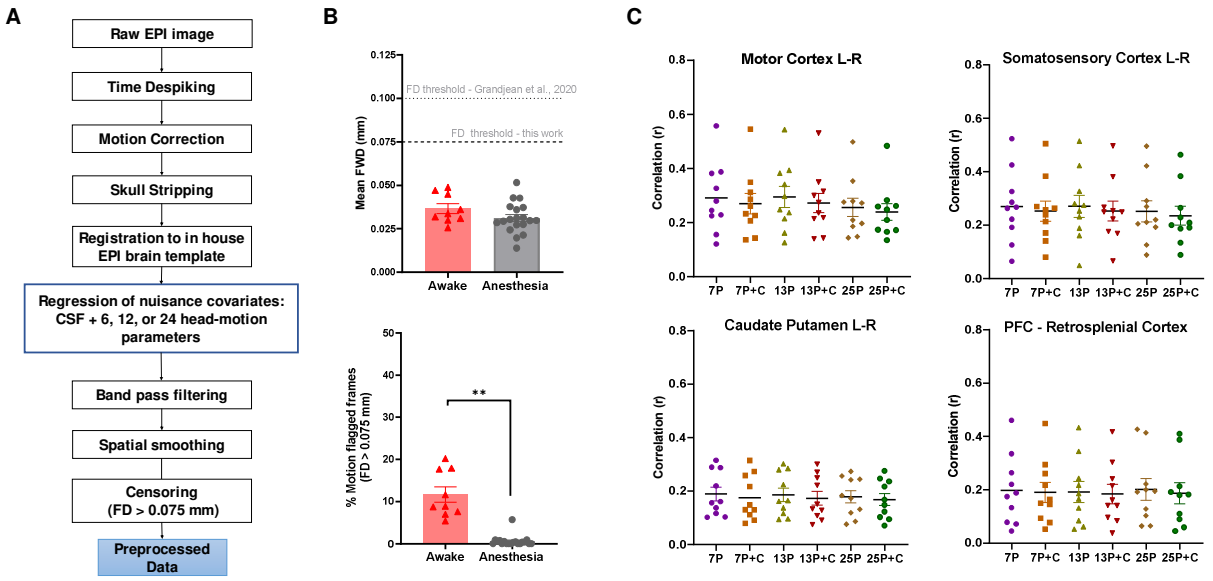

Figure S6. Preprocessing pipeline and denoising strategies. A) The preprocessing steps investigated in our pilot analyses were the use of different head-motion regression parameters (6, 12, or 24), with or without censoring of head-motion flagged frames at a stringent framewise displacement (FD) threshold of 0.075 mm. **B)** Quantification of mean FD (top), and proportion of high FD flagged frames (bottom) in awake and anesthetized (halothane) conditions. **C)** rsfMRI connectivity strength as assessed with a seed-based correlation in awake mice as a function of denoising strategy stringency. As no statistically significant difference in connectivity strength was found across conditions, we opted for the most stringent pipeline assessed (25p + C) for all the analyses of this paper both in awake and anesthetized mice. [7p: regression of CSF and 6 motion parameters; 13P: regression of CSF and 12 motion parameters; 25P: regression of CSF and 24 motion parameters; C: volume censoring].